AGU PUBLICATIONS

JGR

Journal of Geophysical Research: Solid Earth

RESEARCH ARTICLE
10.1002/2017JB014206

Key Points:
- Limited Mg and Ca isotopic fractionation during magmatic process
- Low δ^{26}Mg and $\delta^{44/40}$Ca of Tengchong volcanic rocks are related to ancient carbonates, probably derived from the Indian Oceanic crust
- The species and amount of the recycled carbonates can be constrained by Mg and Ca isotopes

Supporting Information:
- Supporting Information S1

Correspondence to:
Z. Zhang,
zfzhang@gig.ac.cn

Citation:
Liu, F., Li, X., Wang, G., Liu, Y., Zhu, H., Kang, J., … Zhang, Z. (2017). Marine carbonate component in the mantle beneath the southeastern Tibetan Plateau: Evidence from magnesium and calcium isotopes. *Journal of Geophysical Research: Solid Earth*, *122*. https://doi.org/10.1002/2017JB014206

Received 15 MAR 2017
Accepted 12 NOV 2017
Accepted article online 17 NOV 2017

Marine Carbonate Component in the Mantle Beneath the Southeastern Tibetan Plateau: Evidence From Magnesium and Calcium Isotopes

Fang Liu[1,2], Xin Li[1], Guiqin Wang[1], Yufei Liu[1,2], Hongli Zhu[1,2], Jinting Kang[1,3], Fang Huang[3], Weidong Sun[4,5], Xiaoping Xia[1], and Zhaofeng Zhang[1]

[1]State Key Laboratory of Isotope Geochemistry, Guangzhou Institute of Geochemistry, Chinese Academy of Sciences, Guangzhou, China, [2]University of Chinese Academy of Sciences, Beijing, China, [3]Key Laboratory of Crust-Mantle Materials and Environments, School of Earth and Space Sciences, University of Science and Technology of China, Hefei, China, [4]Center of Deep Sea Research, Institute of Oceanography, Chinese Academy of Sciences, Qingdao, China, [5]CAS Center for Excellence in Tibetan Plateau Earth Sciences, Chinese Academy of Sciences, Beijing, China

Abstract Tracing and identifying recycled carbonates is a key issue to reconstruct the deep carbon cycle. To better understand carbonate subduction and recycling beneath the southeastern Tibetan Plateau, high-K cal-alkaline volcanic rocks including trachy-basalts and trachy-andesites from Tengchong were studied using Mg and Ca isotopes. The low δ^{26}Mg (-0.31 ± 0.03‰ to -0.38 ± 0.03‰) and $\delta^{44/40}$Ca (0.67 ± 0.07‰ to 0.80 ± 0.04‰) values of these volcanic rocks compared to those of the mantle (-0.25 ± 0.07‰ and 0.94 ± 0.05‰, respectively) indicate the incorporation of isotopically light materials into the mantle source, which may be carbonate-bearing sediments with low δ^{26}Mg and $\delta^{44/40}$Ca values. In addition, no correlations of δ^{26}Mg and $\delta^{44/40}$Ca with either SiO_2 contents or trace element abundance ratios (e.g., Sm/Yb and Ba/Y) were observed, suggesting that limited Mg and Ca isotopic fractionation occurred during cal-alkaline magmatic differentiation. A binary mixing model using Mg–Ca isotopes shows that 5–8% carbonates dominated primarily by dolostone were recycled back into the mantle. Since Tengchong volcanism is still active and probably related to ongoing plate tectonic movement, we propose that the recycled carbonates are derived from oceanic crust related to the ongoing subduction of the Indian plate.

1. Introduction

Carbon in the form of carbonate in sediments and altered oceanic crust is continuously recycled into the Earth's interior by subduction, where it can then be transferred back to shallow depths by melting and mantle convection and finally degassed to the atmosphere by volcanism (e.g., Alt & Teagle, 1999; Berner et al., 1983; Dasgupta & Hirschmann, 2010; Dasgupta et al., 2004; Sleep & Zahnle, 2001). Kelemen and Manning (2015) suggested that the input of carbon from subduction zones is greater than output from arc volcanoes plus diffuse venting, and most subducting carbon is stored in the mantle lithosphere and crust, while there are also a certain amount of carbon delivered into convecting mantle. Therefore, tracking the fingerprint of recycled carbonate in the Earth's mantle is important for reconstructing deep carbon cycle and clarifying its role in modifying the chemical composition of the mantle.

Magnesium and calcium are two major constituent cations in oceanic carbonate. Their isotopic variations in mantle-derived rocks may shed new light on the carbonate recycling process. Mg isotope fractionation is limited during igneous differentiation (e.g., S. A. Liu et al., 2010; Teng, Li, Rudnick, et al., 2010; Teng et al., 2007; W. Y. Li et al., 2010) and metamorphic dehydration (e.g., Teng et al., 2013; Wang, Teng, & Li, 2014; W. Y. Li et al., 2014) if no recycled materials were involved. In contrast, Mg isotopes can fractionate significantly during carbonate deposition where it ranges from -5.5 to -0.2‰ (Teng, 2017, and references therein), which is significantly lower than the δ^{26}Mg of average upper mantle (-0.25 ± 0.07‰; Bourdon et al., 2010; Handler et al., 2009; Teng, Li, Rudnick, et al., 2010; Yang et al., 2009). Dolomite-rich carbonates can retain their initial light Mg isotopic composition during slab subduction (Wang, Teng, Li, & Hong, 2014). As for Ca isotopes, considerable fractionation can also occur during carbonate precipitation, leading to distinctive Ca isotopic compositions between mantle and marine carbonates. Compared with the $\delta^{44/40}$Ca of the fertile mantle (0.94 ± 0.05‰; Kang et al., 2017), ancient marine carbonates have lower $\delta^{44/40}$Ca (mostly <0.5‰; e.g., Fantle & DePaolo, 2005; Farkaš, Böhm, et al., 2007; Farkaš, Buhl, et al., 2007). For example,

Huang et al. (2011) attributed the light Ca isotopic compositions (0.75 to 1.02‰) in Hawaiian basalts to 4% ancient carbonate component in the Hawaii plume. Thus, the distinctive isotopic offset between mantle and oceanic carbonates makes Mg and Ca isotopes useful tools for tracing subducted carbonates.

Ca-rich carbonate (e.g., limestone) and Mg-rich carbonate (e.g., dolostone) are the two end-members of marine carbonates. Because of their distinctive MgO and CaO contents, different species of marine carbonate would theoretically impose different Mg–Ca isotopic effects on mantle-derived rocks, such that the combination of Mg and Ca isotopes can quantitatively constrain the species of subducted carbonate.

Here we apply Mg and Ca isotopes to trace carbonate recycling in Tengchong volcanic rocks located in the southeastern Tibetan Plateau. Previous lithological and Nd–Sr–Pb isotopic studies have suggested that a subducted slab was involved in the mantle source region of Tengchong volcanic rocks (e.g., B. Q. Zhu et al., 1983; F. Chen et al., 2002; F. Wang et al., 2006; X. Li & Liu, 2012) and that their mantle source was metasomatized by a component derived from clay sediments or mudstones based on U-series disequilibrium and ultra-high Th/U in the volcanic rocks (Zou et al., 2014). Geophysical and seismological studies also revealed high-velocity anomalies in the mantle transition zone, which possibly indicate a stagnant slab under the Tengchong mantle source (Lei et al., 2009, 2013; Wei et al., 2012; Z. Huang et al., 2015). These observations imply that subducted sediments or crust were recycled into the mantle source but were unable to identify the constituting components of the recycled material (e.g., carbonate). In this study, we present high-precision Mg and Ca isotopic analyses, together with major and trace element abundances and Sr–Nd isotopic compositions, to trace recycled carbonates and further constrain the tectonic history of the Tengchong block. Our results show that both δ^{26}Mg and $\delta^{44/40}$Ca of Tengchong volcanic rocks are lower than those of the average mantle, which likely resulted from the incorporation of carbonate into their mantle source.

2. Geological Setting and Samples

The Tengchong volcanic field is an extension of the Lhasa terrane to the southeast, and is bounded by the Bangong–Nujiang suture and the Indus–Tsangpo suture in southwest China (Figure 1a). In southwest China and Burma, the tectonic structure is dominated by N-S and E-NE trending strike-slip faults (Figure 1b). The basement rocks are mainly composed of Paleozoic gneisses and migmatites, Carboniferous sandstones, and late Mesozoic to Cenozoic granitoids (e.g., F. Chen et al., 2002; Zou et al., 2010).

Active Tengchong volcanism commenced at about 5 Ma and has continued to the present (e.g., B. Q. Zhu et al., 1983). Volcanic eruptions in Tengchong were grouped into four different stages (T. F. Chen, 2003; X. W. Huang et al., 2013; Yu et al., 2012): (1) middle-late Pliocene (N_2), mainly composed of olivine basalt; (2) early Pleistocene (Q_1), andesite and dacite; (3) middle Pleistocene (Q_3^{1b}, Q_3^{2b}), basalt and andesite; and (4) Holocene (Q_4^{1b}, Q_4^{2b}), mainly composed of andesite. Heikongshan, Dayingshan, and Ma'anshan volcanoes in Tengchong are considered to have erupted during the Holocene. The latest volcanism occurred in 1609 at Dayingshan, which was recorded by the geographer Xu in the Ming Dynasty. In this study, 19 samples were collected, and sampling locations are shown in Figure 1c. They can be divided into two groups, namely trachy-basalts (Group I) and trachy-andesites (Group II). All samples show porphyritic texture with phenocrysts of pyroxene, olivine, and plagioclase (Figure S1 in the supporting information; X. Li & Liu, 2012; Y. T. Zhang et al., 2012; Zhou et al., 2012).

3. Analytical Methods

3.1. Major and Trace Elements

Rocks were powdered to 200 mesh in an agate mortar for elemental and isotopic analyses. Whole-rock major and trace elements were measured at the State Key Laboratory of Isotope Geochemistry (SKLaBIG), Guangzhou Institute of Geochemistry (GIG), Chinese Academy of Sciences (CAS). Major elements were measured by X-ray fluorescence with relative standard deviation of $<$5%. Reference materials, DZE-2, GSR-1, GSR-2, GSR-3, GSR-4, and GSR-5, were chosen as external calibration standards for calculating the element concentrations, and their results are displayed in Table S1. Trace elements were determined using inductively coupled plasma mass spectrometry (ICP-MS). Analytical procedures were described in detail by J. L. Chen et al. (2010). Table S2 lists the results of trace elements of three USGS reference materials, showing good agreement with the recommended values. The analytical precision and accuracy are better than 10%.

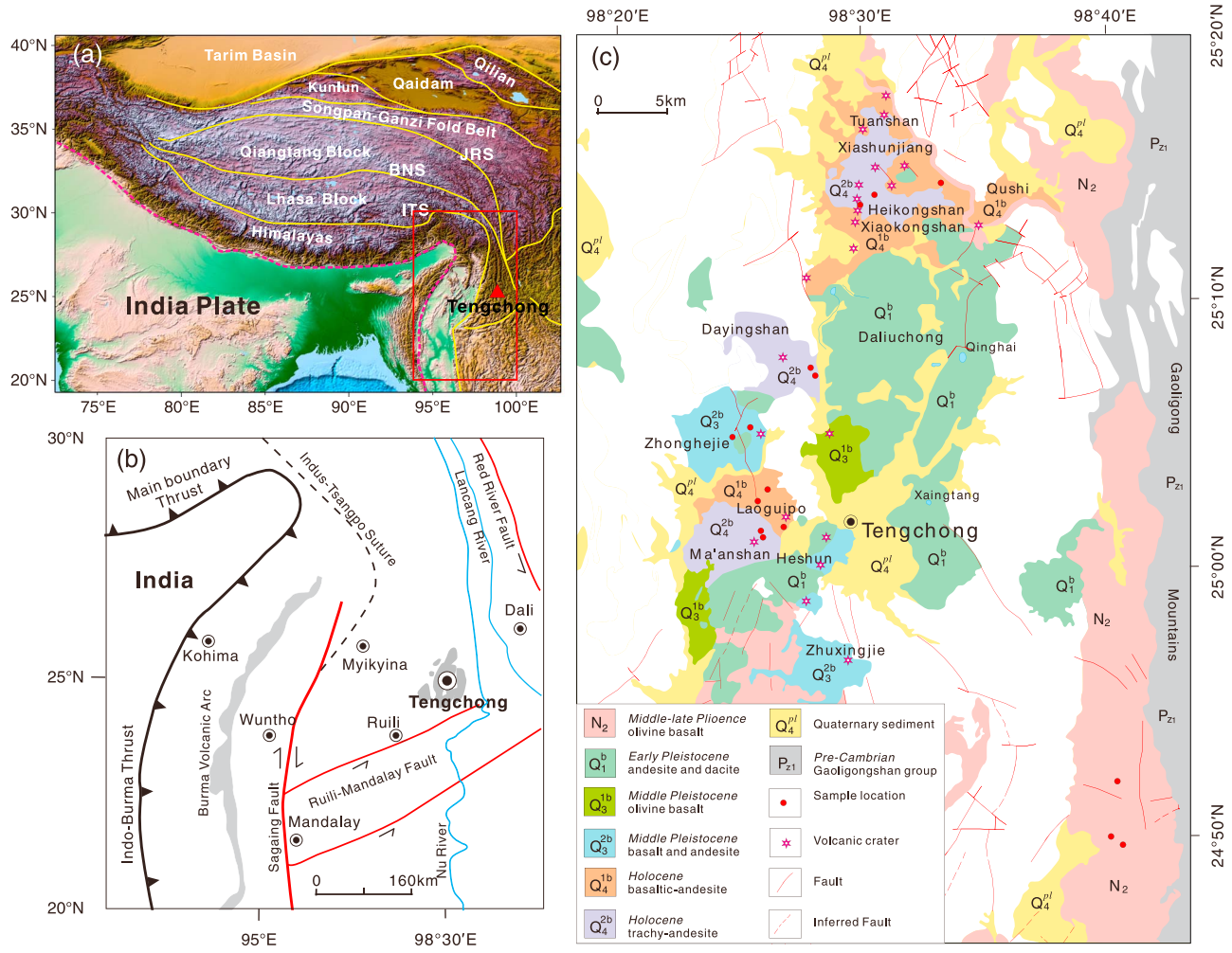

Figure 1. Geological setting of Tengchong area. (a) Regional map of the Tibetan plateau. Yellow lines represent the tectonic boundaries and sutures, ITS is Indus-Tsangpo suture, BNS is Bangong–Nujiang suture, and JRS is Jinsha River suture. Dashed red lines are plate boundaries. Red triangle (98°30′E, 25°N) is the center of the Tengchong volcanic complex. (b) Location map of the Tengchong volcanic field and adjacent areas, modified from B. Q. Zhu et al. (1983). (c) Geological map showing the distribution of volcanic rocks in Tengchong.

3.2. Magnesium Isotopes

Sample digestion was carried out in a class 100 clean laboratory environment at the SKLaBIG, GIG, CAS. About 50 mg of rock powder was weighted into a 7 mL Savillex screw-top beaker. The sample was covered with a mixture of 3:1 concentrated HF:HNO_3 at 100°C for 1 week and then dried down on a hotplate at 100°C. In order to totally break down insoluble CaF_2, the solution was dried down several times with 3 *N* HCl and once with concentrated HNO_3. Finally, the sample was redissolved in 2 mL of 3 *N* HCl for preparation of element purification and isotope determination.

An aliquot containing ~50 μg Mg was dissolved in 0.1 mL of 1 *N* HNO_3. Then it was loaded into a column filled with 1.25 mL cation exchange resin Bio-Rad AG50W-X8 (200–400 mesh). The method follows the established procedure described in An et al. (2014). Eluant of each sample was carefully checked using ICP-OES to make sure that the yield was above 99%. Magnesium isotopic compositions were measured by the sample-standard bracketing method using a Neptune-Plus MC-ICP-MS in the CAS key Laboratory of Crust-Mantle Materials and Environments at the University of Science and Technology of China (USTC). The Mg isotope ratio is reported relative to the Dead Sea metal Mg standard (DSM-3, Galy et al., 2003): $\delta^x Mg = ((^xMg/^{24}Mg)_{sample}/(^xMg/^{24}Mg)_{DSM\text{-}3} - 1) \times 1{,}000$, where $x = 25$ or 26. The 2 standard deviation (2SD) of the measured $^{26}Mg/^{24}Mg$ ratio is $< \pm 0.05‰$ based on ≥ 4 repeat runs. The total procedural Mg blank was lower than 20 ng, negligible relative to the 50 μg loaded into the column. The standards in this study

Table 1
Mg, Ca, Sr, and Nd Isotopic Compositions of the Volcanic Rocks From Tengchong, SE Tibetan Plateau

Sample	Group	δ^{26}Mg	2SD[a]	δ^{25}Mg	2SD	N[b]	$\delta^{44/40}$Ca	2SE[c]	N	$^{87}Sr/^{86}Sr$	$^{143}Nd/^{144}Nd$	ε_{Nd}[d]
13TC-02B	I	−0.27	0.03	−0.14	0.03	4	0.74	0.10	3	0.707567	0.512401	−4.6
13TC-03	I	−0.43	0.01	−0.21	0.01	4	0.70	0.12	2	0.707969	0.512365	−5.3
Replicate	I	−0.44	0.02	−0.22	0.01	4	0.73	0.03	3			
13TC-04	I	−0.42	0.01	−0.23	0.02	4	0.65	0.05	3	0.707944	0.512360	−5.4
13TC-05	I	−0.36	0.03	−0.19	0.02	4	0.76	0.06	5	0.706450	0.512402	−4.6
13TC-06A	II	−0.31	0.03	−0.17	0.02	4	0.67	0.07	3	0.707592	0.512286	−6.9
13TC-06B	II	−0.34	0.02	−0.19	0.03	4	0.78	0.06	3	0.707593	0.512283	−6.9
13TC-06C	II	−0.33	0.03	−0.17	0.01	4	0.73	0.10	3	0.707603	0.512284	−6.9
Replicate	II	−0.33	0.02	−0.17	0.01	4	0.77	0.04	3	0.707583	0.512291	−6.8
13TC-06D	II	−0.34	0.02	−0.17	0.02	4	0.79	0.02	3	0.707594	0.512287	−6.8
13TC-06E	II	−0.34	0.04	−0.17	0.03	7	0.76	0.02	3	0.707615	0.512284	−6.9
13TC-06F	II	−0.36	0.02	−0.18	0.04	4	0.76	0.02	3	0.707645	0.512277	−7.0
13TC-06G	II	−0.36	0.02	−0.19	0.02	4	0.77	0.02	3	0.707543	0.512301	−6.6
13TC-06H	II	−0.35	0.01	−0.18	0.03	4	0.75	0.07	3	0.707517	0.512306	−6.5
13TC-07	I	−0.38	0.04	−0.19	0.03	4	0.78	0.12	2	0.706593	0.512367	−5.3
Replicate	I	−0.36	0.03	−0.18	0.01	4	0.80	0.04	3			
13TC-10	II	−0.35	0.02	−0.17	0.03	4	0.71	0.06	3	0.707545	0.512288	−6.8
13TC-11	II	−0.36	0.02	−0.18	0.01	4	0.77	0.02	3	0.708883	0.512182	−8.9
Replicate	II	−0.32	0.03	−0.16	0.01	4	0.76	0.10	3			
13TC-12A	II	−0.33	0.03	−0.18	0.03	4	0.75	0.07	4	0.708853	0.512184	−8.9
13TC-14	II	−0.32	0.03	−0.15	0.01	4	0.73	0.02	3	0.708550	0.512220	−8.1
13TC-15E	II	−0.31	0.03	−0.16	0.04	3	0.69	0.03	3	0.708533	0.512223	−8.1
13TC-16A	II	−0.38	0.03	−0.20	0.02	4	0.77	0.04	3	0.708555	0.512220	−8.2
Standard												
BHVO-2		−0.26	0.01	−0.14	0.01	4	0.76	0.02	19	0.703521	0.512975	6.6
BCR-2		−0.22	0.02	−0.10	0.03	4				0.705073	0.512641	0.1
Replicate		−0.21	0.04	−0.10	0.04	4						
NBS987										0.710294		
JB-1											0.512787	2.9
JG-1a											0.512393	−4.8
Seawater							1.82	0.03	17			
NIST 915a							0.02	0.02	26			

[a]2SD = 2 standard deviation. [b]N = number for replicate analyses. [c]2SE = 2SD/sqrt(N), standard error. If only once or twice analysis of the sample was available, the error was set as 0.12‰ based on the long-term measurements of seawater. [d]$\varepsilon_{Nd} = (((^{143}Nd/^{144}Nd)_{sample}/(^{143}Nd/^{144}Nd)_{Chondrite} - 1) \times 10{,}000$, $(^{143}Nd/^{144}Nd)_{Chondrite} = 0.512638$.

yielded δ^{26}Mg = −0.26 ± 0.01‰ (2SD, n = 4) for BHVO-2 and −0.22 ± 0.02‰ (2SD, n = 4) for BCR-2 (Table 1), which were consistent with published values within error (e.g., An et al., 2014; Teng et al., 2007, 2015; Teng, Li, Ke, et al., 2010; Teng, Li, Rudnick, et al., 2010).

3.3. Calcium Isotopes

Chemical purification for Ca isotopes follows the procedure described in H. L. Zhu et al. (2016) and F. Liu et al. (2017). Briefly, before Ca purification, an aliquot containing ~50 μg Ca was mixed with an appropriate amount of ^{42}Ca–^{43}Ca double spike solution to make an optimal $^{40}Ca_{sample}$–$^{42}Ca_{spike}$ ratio of 7 (F. Liu et al., 2017). The mixture was then dried down and dissolved in 0.05 mL of 1.6 N HCl. Then it was loaded into a Teflon column packed with 1 mL cation exchange resin Bio-Rad AG MP-50 (100–200 mesh). Ca was rinsed with 1.6 N HCl media, and the column chemistry was carefully calibrated to ensure >99% yield. Calcium isotopic compositions were measured by Triton TIMS at the SKLaBIG, GIG, CAS. ^{41}K was monitored to correct isobaric interference of ^{40}K on ^{40}Ca using $^{40}K/^{41}K = 1.7384 \times 10^{-3}$. Ca isotope data are reported as δ-notation relative to NIST SRM 915a: $\delta^{44/40}Ca = ((^{44}Ca/^{40}Ca)_{sample}/(^{44}Ca/^{40}Ca)_{SRM\ 915a} - 1) \times 1{,}000$. The raw Ca ratios were corrected by ^{42}Ca–^{43}Ca double spike technique using an iterative algorithm with an exponential law adapted from Heuser et al. (2002). NIST SRM 915a, IAPSO seawater, and BHVO-2 were routinely analyzed during the course of an analytical session. The total procedural blanks were 20–70 ng, which were negligible compared to 50 μg Ca loaded into the column. $\delta^{44/40}$Ca is 0.02 ± 0.02‰ (2SE, standard error, n = 26) for NIST SRM 915a, 1.82 ± 0.03‰ (2SE, n = 17) for IAPSO seawater and 0.76 ± 0.02‰ (2SE, n = 19) for BHVO-2 (Table 1), which

are consistent with previous studies (e.g., Amini et al., 2009; Farkaš, Böhm, et al., 2007; Farkaš, Buhl, et al., 2007; Huang et al., 2010; Valdes et al., 2014).

3.4. Strontium and Neodymium Isotopes

Strontium isotopes were analyzed by Triton TIMS at GIG, CAS. Neodymium isotopes were determined using a Neptune Plus MC-ICP-MS at USTC. Analytical methods were described by J. L. Chen et al. (2010) and Xu et al. (2002). Instrument-related isotope bias was corrected using $^{88}Sr/^{86}Sr = 8.375209$ and $^{146}Nd/^{144}Nd = 0.7219$. The $^{87}Sr/^{86}Sr$ value measured for SRM987 was 0.710294 ± 6 (2SE), and $^{143}Nd/^{144}Nd$ value for JNdi was 0.512115 ± 6 (2SE). The BHVO-2 and BCR-2 yielded average $^{87}Sr/^{86}Sr$ = 0.703521 ± 5 (2SE) and 0.705073 ± 8 (2SE), respectively. The standard BHVO-2, BCR-2, JG-1a, and JB-1 gave $^{143}Nd/^{144}Nd = 0.512975 \pm 4$ (2SE), 0.512641 ± 4 (2SE), 0.512393 ± 3 (2SE), and 0.512787 ± 4 (2SE), respectively. All results are presented in Table 1.

4. Results

Major and trace element compositions of Tengchong volcanic rocks are reported in Table S3. Five samples, including 13TC-02B, 13TC-03, 13TC-04, 13TC-05, and 13TC-07, are classified as trachy-basalts (Group I); other samples are trachy-andesites (Group II). Within Group I samples, 13TC-02B, 13TC-03, and 13TC-04 have relatively high loss on ignition (LOI; 2.43 to 3.35 wt.%), which suggests post-alteration processes, while others are fresh with LOI close to zero. For Group I samples, SiO_2 contents vary from 50.8 wt.% to 53.4 wt.%, and K_2O contents range from 1.7 wt.% to 2.7 wt.%. For Group II samples, SiO_2 contents range from 57.3 wt.% to 61.6 wt.%, and they are potassium-rich with K_2O ranging from 3.3 wt.% to 4.1 wt.%.

The LREE and LILE enrichment in Group II is greater than Group I (Figure S2). Both Group I and Group II samples show enrichment of LREE and display positive Pb anomalies and negative Nb, Ta, and Ti anomalies (Figure S2), consistent with previous studies (Gao et al., 2015; Y. T. Zhang et al., 2012; Zhou et al., 2012; Zou et al., 2014). They have high $^{87}Sr/^{86}Sr$ (0.706450 to 0.708883) and low ε_{Nd} (−4.6 to −8.9) signatures (Table 1), within the range of reported data in previous studies (e.g., B. Q. Zhu et al., 1983; F. Chen et al., 2002; Zou et al., 2014). Fresh volcanic rocks have ultra-high Th/U ratios, ranging from 8.5 to 10.5 (Table S3), even higher than some well-known high Th/U lavas, such as the Gaussberg lavas (7.55 ± 0.05, Williams et al., 1992).

Mg and Ca isotopic compositions are listed in Table 1. Group II samples have a narrow range of $\delta^{26}Mg$ from −0.31 ± 0.03‰ (2SD, $n = 4$) to −0.38 ± 0.03‰ (2SD, $n = 4$) with an average of −0.34 ± 0.04‰ (2SD, $n = 14$). Of the altered samples with high LOI in Group I, 13TC-02B has the highest $\delta^{26}Mg$ (−0.27 ± 0.03‰, $n = 4$), while 13TC-03 and 13TC-04 show the lowest $\delta^{26}Mg$ values (average = −0.43‰). $\delta^{26}Mg$ of the fresh Group I samples (13TC-05 and 13TC-07) are similar with that of Group II. Although these volcanic rocks have variable CaO contents from 4.65 to 7.99 wt.%, they exhibit relatively homogenous Ca isotopic compositions with $\delta^{44/40}Ca$ from 0.67 to 0.80‰. The variation of $\delta^{44/40}Ca$ is only 0.13‰, which falls within the analytical precision of ±0.12‰ (2SD).

5. Discussion

The relatively high LOI in 13TC-02B, 13TC-03, and 13TC-04 (2.43–3.35 wt.%, Table S3) suggests that they have experienced low-temperature alteration. During alteration, these samples could experience element migration and isotope fractionation, especially for Mg and Ca. Thus, these three samples are excluded, and only 13TC-05 and 13TC-07 in Group I are used for further discussion about their source composition. All Group I and Group II samples show similar chondrite-normalized REE diagrams, primitive mantle-normalized trace elements patterns (Figure S2; McDonough & Sun, 1995), and consistent evolution trends (Figure S1). Therefore, we conclude that they are derived from the same mantle source.

Magnesium isotopic compositions of the Tengchong volcanic rocks (−0.31 to −0.38‰) are slightly beyond the range of typical oceanic basalts (−0.18 to −0.32‰; Teng, Li, Rudnick, et al., 2010). Similarly, their $\delta^{44/40}Ca$ values (0.67 to 0.80‰) are systematically lower than the fertile mantle (0.94 ± 0.05‰; Kang et al., 2017). These isotopic signatures can possibly be attributed to several processes, such as source heterogeneity, magmatic

processes, crustal contamination, and alteration. In the following, we first evaluate the process responsible for the light Mg and Ca isotopic compositions and then discuss their origin and geodynamic implications.

5.1. Effect of Shallow Level Processes

Low-temperature alteration like chemical weathering can significantly fractionate the Mg and Ca isotopic compositions of volcanic rocks (e.g., D. Liu et al., 2014; Ewing et al., 2008; Jacobson et al., 2015; K. J. Huang et al., 2012; Pogge von Strandmann et al., 2008; Teng, Li, Ke, et al., 2010; Tipper et al., 2008). The three altered samples, 13TC-02B, 13TC-03, and 13TC-04, display considerable deviations in δ^{26}Mg (-0.27 ± 0.03‰ to -0.44 ± 0.02‰) and insignificant differences in $\delta^{44/40}$Ca (0.65 ± 0.05‰ to 0.74 ± 0.10‰; Table 1).

High-K calc-alkaline rocks in Tengchong have high $^{87}Sr/^{86}Sr$ and low ε_{Nd} (Table 1). However, these features do not reflect crustal contamination. F. Chen et al. (2002) suggested that the large Pb–Sr isotopic deviations between the country rocks and the volcanic rocks did not support significant crustal contamination. Zou et al. (2014) proposed that the absence of xenocrystic zircons older than 300,000 years indicates negligible effect of crustal contamination during the magma ascent. In addition, because the continental crust is marked with high Sr content and high $^{87}Sr/^{86}Sr$ while the mantle has low Sr content and low $^{87}Sr/^{86}Sr$, a linear correlation between 1/Sr and $^{87}Sr/^{86}Sr$ should be observed if crustal contamination occurred. However, no such correlation is found in our samples. Moreover, the remarkably high Th content and Th/U ratios (up to 10.5) preclude crustal assimilation because of the low Th content and Th/U of granulitic xenoliths (Table S3; F. Wang et al., 2006). Therefore, we conclude that the light Mg and Ca isotopic compositions of the fresh Tengchong volcanic rocks are unlikely to be related with shallow level processes.

5.2. Mg and Ca Isotope Fractionation During Magmatic Processes

5.2.1. Fractional Crystallization

Tengchong volcanic rocks have experienced significant fractional crystallization, mainly involving olivine, orthopyroxene, clinopyroxene, plagioclase, and hornblende (Figure S1; e.g., X. Li & Liu, 2012; Y. T. Zhang et al., 2012; Zhou et al., 2012). Yang et al. (2009) showed that there were no measurable Mg isotopic differences between olivine, orthopyroxene, and clinopyroxene in peridotite. S. A. Liu et al. (2010) suggested that hornblende and biotite in granitoids displayed similar Mg isotopic compositions. The limited intermineral fractionation probably reflects the same coordination number of Mg (CN = 6) in these rock-forming minerals. Thus, fractional crystallization of these minerals is not expected to cause Mg isotope variation in evolved magmas. Our samples display no correlations between δ^{26}Mg and SiO_2 content (Figure 2a), implying that magma differentiation did not lead to measurable Mg isotope fractionation. This is in accordance with previous studies that suggest limited Mg isotope fractionation occurs during basalt and granite differentiation (S. A. Liu et al., 2010; Teng et al., 2007; W. Y. Li et al., 2010).

With respect to Ca isotopes, the relatively heavy isotopic signatures of olivine and orthopyroxene (Huang et al., 2010; Kang et al., 2016) do not significantly affect bulk $\delta^{44/40}$Ca because of their low abundance of CaO (usually <0.05 wt.% in olivine and <1 wt.% in orthopyroxene) compared to that of the whole rock (~6.0 wt.%, Table S3). On the other hand, clinopyroxene, plagioclase, and hornblende are isotopically identical with the host volcanic rocks (Kang et al., 2016; Skulan et al., 1997), suggesting that the crystallization of these minerals has limited effect on Ca isotope fractionation. Assuming that fractional crystallization can fractionate Ca isotopes, large isotopic variation should be observed in basalts. However, $\delta^{44/40}$Ca of mafic rocks are not correlated with their Ca or Mg contents (Amini et al., 2009; F. Liu et al., 2017). Moreover, $\delta^{44/40}$Ca of Tengchong volcanic rocks show no correlations with SiO_2 (Figure 2b), which also indicates limited Ca isotope fractionation during fractional crystallization.

5.2.2. Partial Melting

Previous studies demonstrated that no significant Mg isotope fractionation occurs during mantle melting (Handler et al., 2009; S. A. Liu et al., 2010; Teng et al., 2007; Teng, Li, Rudnick, et al., 2010; W. Y. Li et al., 2010; Yang et al., 2009). This is consistent with the lack of correlation between δ^{26}Mg and trace element ratios, such as Sm/Yb and Ba/Y, which are strongly dependent on the degree of partial melting (Figures 2c and 2e).

In contrast, Ca isotopes may fractionate during mantle melting. Previous studies on mantle minerals show that olivine and orthopyroxene tend to be enriched in heavy Ca isotopes relative to clinopyroxene

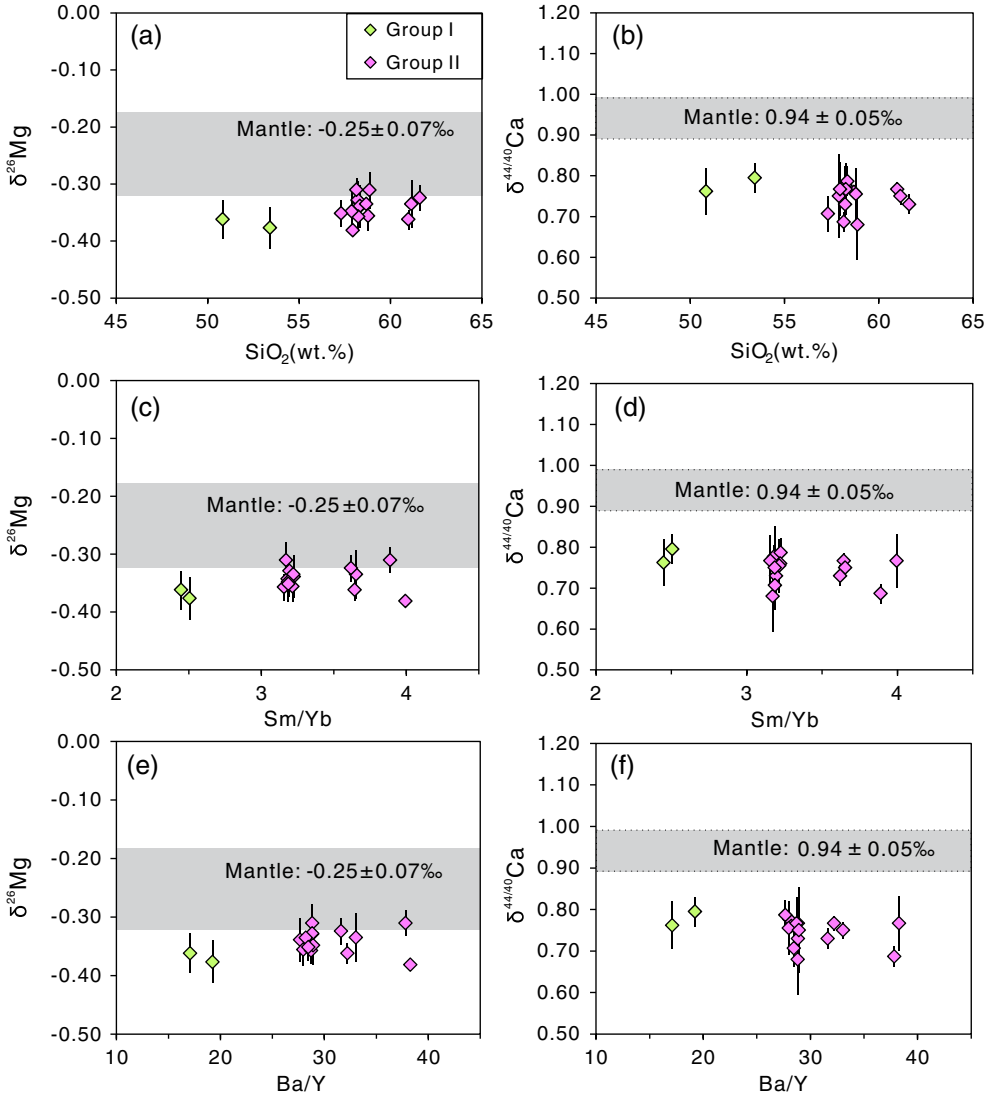

Figure 2. (a, b) δ^{26}Mg or $\delta^{44/40}$Ca versus SiO_2 and (c-d) Sm/Yb and (e-f) Ba/Y in the Tengchong volcanic rocks. Group I are trachy-basalts; Group II are trachy-andesites. Altered samples are not plotted here. Gray bar represents the widely accepted δ^{26}Mg of the mantle (−0.25 ± 0.07‰; Teng, Li, Rudnick, et al., 2010). Dashed gray bar represents the $\delta^{44/40}$Ca of the fertile mantle (0.94 ± 0.05‰; Kang et al., 2017). Sm/Yb and Ba/Y are sensitive to partial melting, which will increase when partial melting degree decreases.

(Huang et al., 2010; Kang et al., 2016). When the mantle experiences partial melting, light Ca isotopes may preferentially enter into melt because clinopyroxene is consumed first (Green, 1973; Jaques & Green, 1980). As reported by Amini et al. (2009) and F. Liu et al. (2017), $\delta^{44/40}$Ca of ultramafic rocks are negatively correlated with CaO and positively correlated with MgO, suggesting that Ca isotopes possibly fractionate during partial melting of mantle peridotite. Recently, Kang et al. (2017) found that $\delta^{44/40}$Ca in moderately depleted peridotites (1.07 ± 0.04‰) from the Siberia craton are slightly higher than in fertile spinel and garnet peridotites (0.94 ± 0.05‰), indicating that light Ca isotopes preferentially partition into melt. Therefore, partial melting of mantle peridotites may cause Ca isotope fractionation. Nevertheless, the influence of subsequent magmatic differentiation seems to be insignificant. This is supported by the following evidence: (1) No $\delta^{44/40}$Ca deviations were observed for mafic rocks despite a wide range of Ca contents (Amini et al., 2009; F. Liu et al., 2017); (2) As for our data, there are no relationships between $\delta^{44/40}$Ca and Sm/Yb and Ba/Y (Figures 2d and 2f). According to recent estimations from Kang et al. (2017), partial melting of fertile mantle can produce observable isotope fractionation at melting degree ≥10%. The degree of partial melting of Tengchong volcanic rocks, however, has already been demonstrated to be only ~5% (Zhou et al., 2012), which can only result in shifts in $\delta^{44/40}$Ca of less than 0.05‰

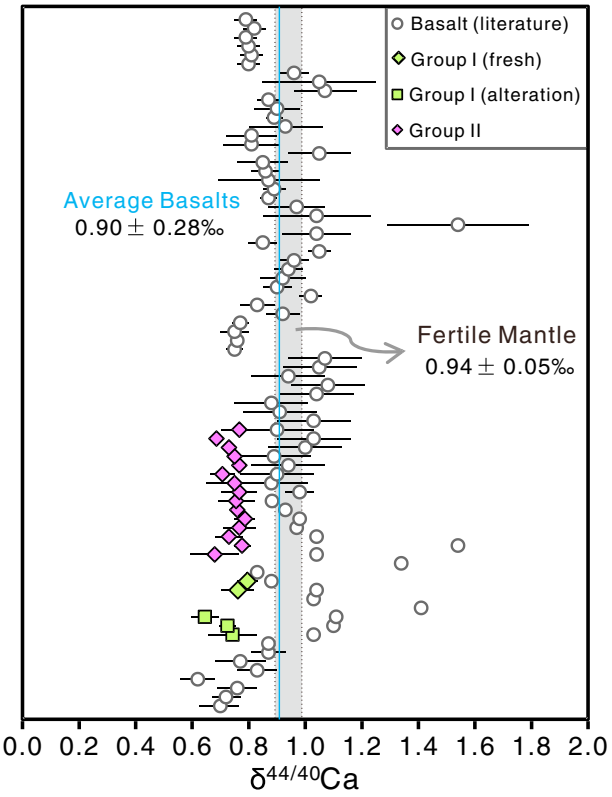

Figure 3. $\delta^{44/40}$Ca values are shown relative to NIST SRM915a. Gray open circles are terrestrial basalts (Amini et al., 2009; Depaolo, 2004; Fantle & Tipper, 2014; Hindshaw et al., 2013; Holmden & Bélanger, 2010; Huang et al., 2010; Jacobson et al., 2015; Simon & Depaolo, 2010; Skulan et al., 1997; Valdes et al., 2014). Blue line represents the average $\delta^{44/40}$Ca of basalts. Gray bars represent the $\delta^{44/40}$Ca of the fertile mantle (Kang et al., 2017). No $\delta^{44/40}$Ca variations were observed between Group I and Group II. Altered samples displayed similar isotopic composition with the fresh samples.

(Kang et al., 2017). In this study, $\delta^{44/40}$Ca of Tengchong volcanic rocks have a narrow variation from 0.67 to 0.80‰ with an average of 0.74 ± 0.08‰, lower than the value of fertile mantle (0.94 ± 0.05‰; Kang et al., 2017) by nearly 0.2‰. This 0.2‰ offset cannot be caused by partial melting but should be related to the mantle source. Additionally, as illustrated in Figure 3, our data are systematically lower than the average $\delta^{44/40}$Ca of basalts (0.90 ± 0.28‰; Amini et al., 2009; DePaolo, 2004; Fantle & Tipper, 2014; Hindshaw et al., 2013; Holmden & Bélanger, 2010; Huang et al., 2010; Jacobson et al., 2015; Simon & DePaolo, 2010; Skulan et al., 1997; Valdes et al., 2014), which may indicate that the mantle source beneath Tengchong has isotopically lighter material. Therefore, we conclude that the effect of partial melting on $\delta^{44/40}$Ca is small (~0.05‰ or less) in Tengchong volcanic rocks, and their mantle source may be metasomatized by isotopically light components.

5.3. The Origin of Low δ^{26}Mg and $\delta^{44/40}$Ca Volcanic Rocks

5.3.1. Low δ^{26}Mg and $\delta^{44/40}$Ca Induced by Carbonate Metasomatism

Given the limited Mg and Ca isotope fractionation during shallow processes and magmatic processes, the most likely mechanism to cause the low δ^{26}Mg and $\delta^{44/40}$Ca in the Tengchong volcanic rocks is that the mantle source incorporated isotopically light components. Several geochemical observations suggest that the Tengchong mantle source incorporates recycled marine sediments. First, Tengchong volcanic rocks have ultra-high Th/U ratios (vary from 8.5 to 10.5; Table S3), which are closely related to metasomatism by components from subducted marine sediments (F. Wang et al., 2006; Prelević et al., 2013; Sekine & Wyllie, 1983). The Th/U ratios of sediments vary from less than 1 to greater than 10 due to their different geochemical behaviors in marine system (Plank & Langmuir, 1998). Slab-derived fluids are enriched in U relative to Th, and thus, the ultra-high Th/U ratios may not reflect significant fluid additions. Instead, high Th/U ratios reflect a mature and weathered source, such as clay-rich sediments (Plank & Langmuir, 1998; Zou et al., 2014). Secondly, Tengchong volcanic rocks have high Th/Yb (5–13) and low Ba/La (11–15), indicating the input of sediment or sediment melts rather than slab-derived fluids into the mantle source (Sun et al., 2004; Woodhead et al., 2001; X. M. Liu et al., 2014). Additionally, the high Pb (12.8–28.9 ppm) and low Ce/Pb (4.7–6.3) also suggest the addition of sediments into the mantle. Finally, Nd isotopes can be effectively used to trace the addition of sediments (e.g., Hawkesworth et al., 1997), and the good negative relationships between ε_{Nd} and Th/Nd and Th/Nb (Figure 4) illustrate that sediments have been recycled into the mantle.

Marine sediments could contain a significant fraction of carbonates. If the mantle source was previously metasomatized by carbonatite melts derived from recycled sediments, the so-called "carbonatite fingerprints" should be observed in volcanic rocks (Bizimis et al., 2003; Hoernle et al., 2002), which is characterized by superchondritic Zr/Hf ratios (40–44; Table S3). In general, carbonates have extremely light Mg (Teng, 2017, and references therein) and Ca (e.g., Fantle & DePaolo, 2005; Farkaš, Böhm, et al., 2007; Farkaš, Buhl, et al., 2007; Tipper et al., 2006) isotopic compositions. The MgO content of dolostone can be up to 20 wt.%, which is comparable to the depleted mantle (MgO = ~38 wt.%; Workman & Hart, 2005). The CaO content of the depleted mantle is about 3 wt.% (Workman & Hart, 2005), while the CaO content of carbonates can be up to 56 wt.%. Therefore, recycling carbonate-bearing sediments into the mantle will likely decrease δ^{26}Mg and $\delta^{44/40}$Ca of the volcanic rocks (e.g., Ke et al., 2016). The low δ^{26}Mg and $\delta^{44/40}$Ca observed in Tengchong volcanic rocks are most likely related to the incorporation of recycled carbonate component into the mantle source of Tengchong volcanic rocks.

5.3.2. Species and Amount of the Recycled Materials

Many different isotopes have been previously applied to evaluate the amount and composition of carbonates recycled into mantle source regions. For example, Huang et al. (2011) combined Ca and Sr isotopes

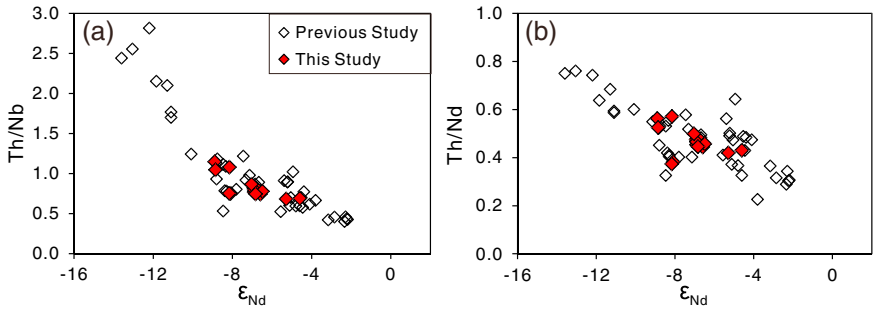

Figure 4. ε_{Nd} versus Th/Nb and Th/Nd for Tengchong volcanic rocks. Good negative relationships reflect that sediments were involved into the depleted mantle. Red rhombus represent samples reported in this study, and others were reported in previous studies (e.g., Gao et al., 2015; X. Li & Liu, 2012; Y. T. Zhang et al., 2012; Zhou et al., 2012; Zou et al., 2014).

to trace recycled carbonates and proposed that the addition of 4% ancient carbonates into the Hawaiian source could explain the variation of $\delta^{44/40}$Ca in Hawaiian shield lavas. D. Liu et al. (2015) identified carbonatite metasomatism using Mg–Sr–Os isotopes and suggested that the variably low δ^{26}Mg of Tibetan ultrapotassic rocks could be attributed to carbonate-bearing sediments. Mg–Sr–O isotopes were employed to study the origin of syenites from northwest Xinjiang, China, showing that syenites with low δ^{26}Mg were caused by the incorporation of dolostone, limestone, and Indian sediment (Ke et al., 2016). In the modeling of Mg and Sr isotopes, S. G. Li et al. (2017) suggested that 1–10% recycled carbonates were responsible for the low δ^{26}Mg anomaly of the continental basalts (<110 Ma) in eastern China. However, to date, there is no work simultaneously using Mg and Ca isotopes to study the recycling carbonate components in the mantle source. Here we attempted to quantitatively identify the composition of materials that subducted into the mantle beneath Tengchong area through Mg and Ca isotopes.

Recycled sediments consist of carbonates, pelagic or red clays, and muds (Plank & Langmuir, 1998). Since carbonate is an important Mg and Ca carrier and generally characterized with light Mg and Ca isotopes, deep recycling of carbonates is potentially inducing heterogeneity of Mg and Ca isotopic composition in the mantle. Both calcite and dolomite show lighter Mg and Ca isotopic compositions compared with fertile mantle, yet calcite has lower MgO but higher CaO contents. Therefore, individual mantle sources metasomatized by melts derived from recycled materials with different carbonate phases (e.g. calcite and dolomite) will have different Mg and Ca isotopic compositions, which were then imprinted on corresponding magmas. In order to constrain the species of carbonate involved in the mantle source, we make a simple two end-member mixing model between the mantle and carbonates using Mg–Ca isotopic compositions (Table 2; Figure 5). In this modal calculation, $\delta^{44/40}$Ca of the depleted mantle is set as 1.00 ± 0.05‰ following the study of Kang et al. (2017). Kang et al. (2017) defined the $\delta^{44/40}$Ca of the fertile mantle as 0.94 ± 0.05‰, while the average of $\delta^{44/40}$Ca of moderately refractory peridotites was 1.07 ± 0.05‰ at melting degree ≥20%. Although we can estimate the degree of partial melting of the Tengchong volcanic rocks (~5%; Zhou et al., 2012), the

Table 2
Parameters for Model Calculations

	δ^{26}Mg	MgO (wt.%)	$\delta^{44/40}$Ca	CaO (wt.%)	$^{87}Sr/^{86}Sr$	Sr (ppm)	ε_{Nd}	Nd (ppm)
DMM[a]	−0.25	38	1.00	3.17	0.70263	7.7	9.6	0.581
Dolostone[b]	−3.4	21.7	0.4	30				
Limestone[c]	−3.4	0.5	0.4	56				
Carbonate[d]	−3.4	15.3	0.4	37.8	0.707	1,285	−10	13
Clay sediments[e]	−0.05	2.8	0.6	2.5	0.720	230	−14	70

[a]DMM denotes the depleted mantle. Database: δ^{26}Mg, Teng, Li, Rudnick, et al. (2010); $\delta^{44/40}$Ca, Kang et al. (2017); other data are from Workman and Hart (2005). [b]δ^{26}Mg of dolostone is the average Mg isotopic composition of sedimentary carbonates (Teng, 2017, and references therein). $\delta^{44/40}$Ca of dolostone is assumed to be 0.4‰ (e.g., Farkaš, Böhm et al., 2007; Farkaš, Buhl et al., 2007). MgO and CaO contents are calculated assuming that chemical formula of dolostone is $(Ca_{0.5}Mg_{0.5})CO_3$. [c]δ^{26}Mg and $\delta^{44/40}$Ca of limestone are evaluated to be the same as dolostone. MgO is assumed to be low. CaO is calculated by assuming that limestone consists of pure carbonate. [d]Carbonate is supposed to be composed of dolostone and limestone. The proportion between dolostone and limestone is varied; here we set it as 0.7:0.3. Sr and Nd are from Plank and Langmuir (1998). [e]Clay sediments are complex mixtures, including clay and mud. δ^{26}Mg is the average value of sediments from W. Y. Li et al. (2010). $\delta^{44/40}$Ca is estimated to be 0.6 (Fantle & DePaolo, 2005). Other data are estimated from Plank and Langmuir (1998) and Richards et al. (2005).

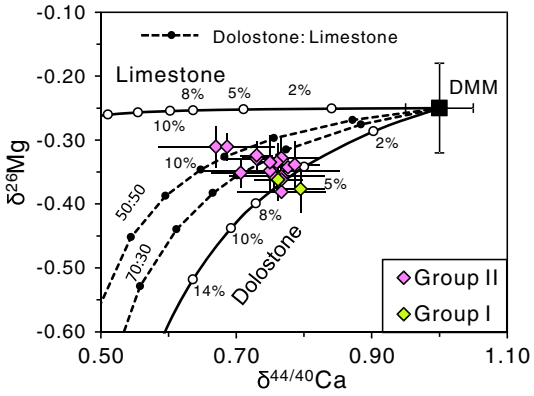

Figure 5. Mg–Ca isotopes mixing model of the depleted MORB mantle (DMM), limestone, and dolostone. The labels on dashed curves are ratios of dolostone to limestone. The percentage label on the curve is the proportion of limestone or dolostone. Altered samples are not plotted here. Parameters and data source are listed in Tables 1 and 2.

nature of peridotite in their mantle source (refractory or fertile) is unknown, so we adopt a medium value (1.00 ± 0.05‰) to represent the isotopic composition of depleted mantle. According to our calculation, the different values ($\delta^{44/40}$Ca vary from 0.94 to 1.07‰) of the depleted mantle will make little difference to the modeling results. As illustrated in Figure 5, the dolostone (with proportions ranging from 50% to 100%) might play a key role in the origin of the low δ^{26}Mg and $\delta^{44/40}$Ca features in Tengchong volcanic rocks. The results show that about 5–8% carbonate was incorporated into the depleted mantle (Figure 5). However, incorporation of carbonates alone cannot explain Sr and Nd isotopic compositions of these samples.

Clastic sediments have low Nd and high Sr isotopic compositions (Plank & Langmuir, 1998), and their $^{87}Sr/^{86}Sr$ can be up to 0.765 (Richards et al., 2005). A small amount of sediments incorporated into the depleted mantle could significantly increase $^{87}Sr/^{86}Sr$ and decrease $^{143}Nd/^{144}Nd$. To further explain and verify the amount of sediments recycled into the mantle, three components (depleted MORB mantle (DMM), clay, and carbonate) are applied in the models (Table 2, Figure 6). $^{87}Sr/^{86}Sr$ and $^{143}Nd/^{144}Nd$ of clay sediments are evaluated with the average values according to Plank and Langmuir (1998) and Richards et al. (2005). In the plots of δ^{26}Mg and $\delta^{44/40}$Ca versus $^{87}Sr/^{86}Sr$ and ε_{Nd} (Figure 6), approximately 5–12% sediments recycled into the depleted mantle could explain the isotope variations, generally consistent with the results of Mg–Ca isotopes mixing model.

Large amounts of carbonates are retained in the slab after subduction dehydration, which can be recycled into the deep mantle at the depth of approximately 300 to 700 km (Kerrick & Connolly, 2001; Poli et al.,

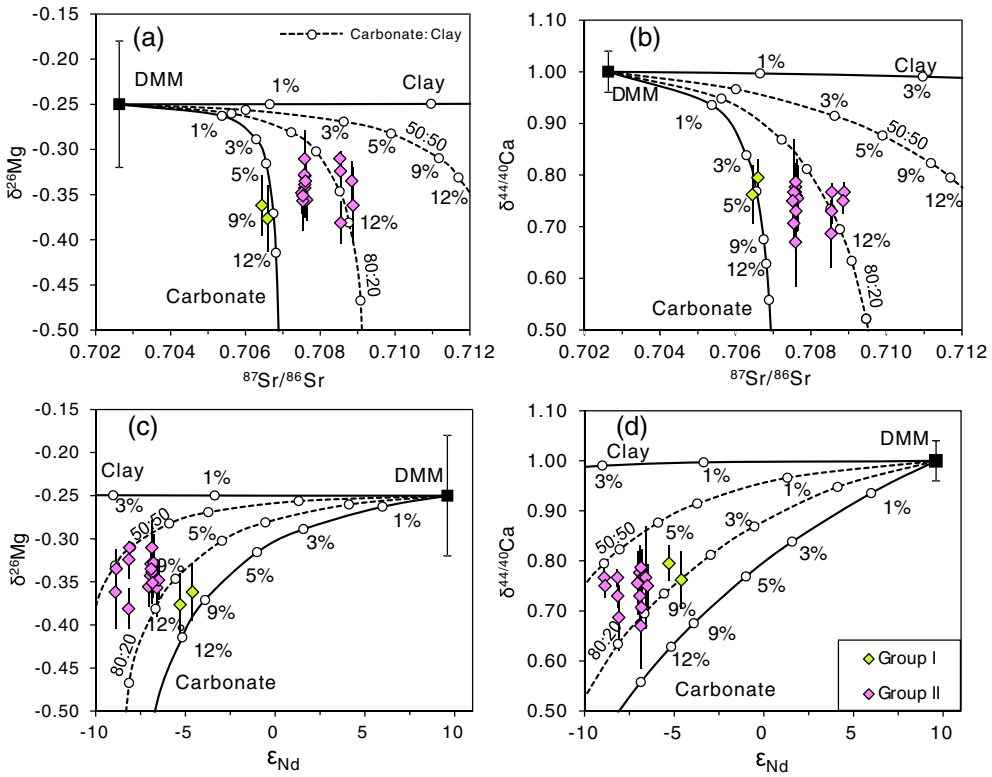

Figure 6. Isotopes mixing models of the DMM, clay, and carbonate. To simplify the calculation, marine sediments are regarded as carbonates plus clay sediments. (a) Mg–Sr, (b) Ca–Sr, (c) Mg–Nd, and (d) Ca–Nd. The labels on the dashed curves are the ratios of carbonate to clay. The percentage label on the curve is the proportion of clay or carbonate involved into the mantle. Altered samples are not plotted here. Parameters and data source are listed in Tables 1 and 2.

2009; Thomson et al., 2016). However, not all species of carbonates can survive beyond slab dehydration, except those that are stable under high *P–T* conditions. To be specific, calcite is unstable at high pressures, but it can be transformed to high-Mg carbonates (e.g., dolomite) through Ca–Mg exchange with silicates (e.g., Dasgupta & Hirschmann, 2010; Kushiro, 1975). On the other hand, Wang, Teng, and Li (2014) suggested that calcite-rich carbonates are unlikely to preserve their initial values to cause local mantle isotope heterogeneity, but dolomite-rich carbonates are more capable to inherit their initial values during subduction. Therefore, Mg-rich carbonate can be significant in the subducted slabs and carried into deep mantle. This is consistent with our modeling calculation that carbonate is mainly composed of dolostone (Figure 5).

The ongoing subduction of Indian Oceanic crust could bring water and sediments to the mantle source region. Mg-rich carbonates (e.g., dolomite), which are shown to be stable under high *P–T* conditions, are also recycled into the mantle transition zone (Thomson et al., 2016). Melting of these carbonate phases, together with some recycled sediments, produces large amounts of aqueous carbonated silicate melts, which rise into overlying mantle, lowering its solidus and triggering further magma formation (e.g., Johnson et al., 2009). Geochemical compositions of the Tengchong volcanic rocks also favor such a complex metasomatic and flux melting process. The enrichment of LILE and other fluid mobile elements (e.g., Rb, Ba, K, U, Th, and LREE) and the depletion of most HFSE (especially Nb and Ta) of these Tengchong samples (Figure S2) strongly suggest recycled crustal components in their mantle source. This may result from additions of LILE and fluid mobile elements through varying proportions of fluids and aqueous carbonated silicate melts into the mantle source (e.g., Kelemen et al., 2003; Wu et al., 2017).

5.4. Geodynamic Implications

We suggest that the light Mg and Ca isotopic compositions of Tengchong volcanic rocks are caused by the incorporation of isotopically light carbonates derived from the subducted slab into their mantle source region. The southeastern Tibetan Plateau suffered from three subduction events, including the Neo-Tethyan Oceanic subduction, the Indian continental subduction, and the Indian Oceanic subduction (e.g., Zhou et al., 2012). Hence, it is necessary to judge which subduction event could provide the carbonates. Guo et al. (2015) proposed that Tengchong lavas were related to the interaction between modern Indian margin sediments and the depleted mantle. However, the relatively low MgO content and the similar δ^{26}Mg of continental crust (Rudnick & Gao, 2003; Teng et al., 2013; Workman & Hart, 2005; Yang et al., 2016) can hardly modify the δ^{26}Mg of the mantle. On the other hand, $\delta^{44/40}$Ca of modern carbonates (0.9‰; e.g., Fantle, 2015; Griffith et al., 2015) cannot affect the mantle's composition significantly due to the small difference in Ca isotopic compositions between them. Thus, the carbonates are most likely derived from the oceanic crust.

On the basis of plate tectonic reconstructions, Neo-Tethyan Oceanic crust was subducted into the mantle beneath Tengchong in the Cretaceous (Hafkenscheid et al., 2006; Van der Voo et al., 1999). Recently, high-resolution seismic and tomographic data showed that a broad low-velocity zone extends down to the 410 km discontinuity with a high-velocity anomaly region at ~660 km (e.g., Lei et al., 2009, 2013; R. Zhang et al., 2017; Wei et al., 2012). The high-velocity region might represent a cold and stagnant slab, probably the Neo-Tethyan Oceanic slab (Figure 7; Zhou et al., 2012). According to modern GPS observations, the India Oceanic plate is currently moving northward with a velocity of 30 mm per year (Figure 7; e.g., Lei et al., 2013), which may account for the ~410 km discontinuity area beneath Tengchong region (Zhou et al., 2012). As shown in Figure 7, the stagnant Neo-Tethyan slab might feed the Tengchong volcanoes, similar to the model of the stagnant Pacific slab feeding the Cenozoic basalts in eastern China (e.g., S. G. Li et al., 2017). However, the active Tengchong volcanism commenced at about 5 Ma (e.g., B. Q. Zhu et al., 1983), delayed more than 50 Ma after India–Asia collision, implying that the trigger for mantle melting cannot be simply attributed to volatile additions related to the subducted Neo-Tethyan Oceanic slab.

The Indian Oceanic crust, particularly the northern end of the Ninetyeast Ridge, is currently being subducted beneath SW China and Burma (Zhou et al., 2012). This ridge is a linear, age-progressive seamount chain in the India Ocean, fed by the Kerguelen plume (Figure 7). The plateau ridge would be more buoyant than adjacent normal oceanic slab, causing a much flatter subduction at the ~410 km discontinuity (Figure 7b). As illustrated in Figure 7, an older portion (115–126 Ma) of the Ninetyeast Ridge was close to the Tengchong area (Figure 7; D. C. Zhu et al., 2009; Frey et al., 2011; Kent et al., 2002; Seno & Rehman, 2011; Storey et al., 1989;

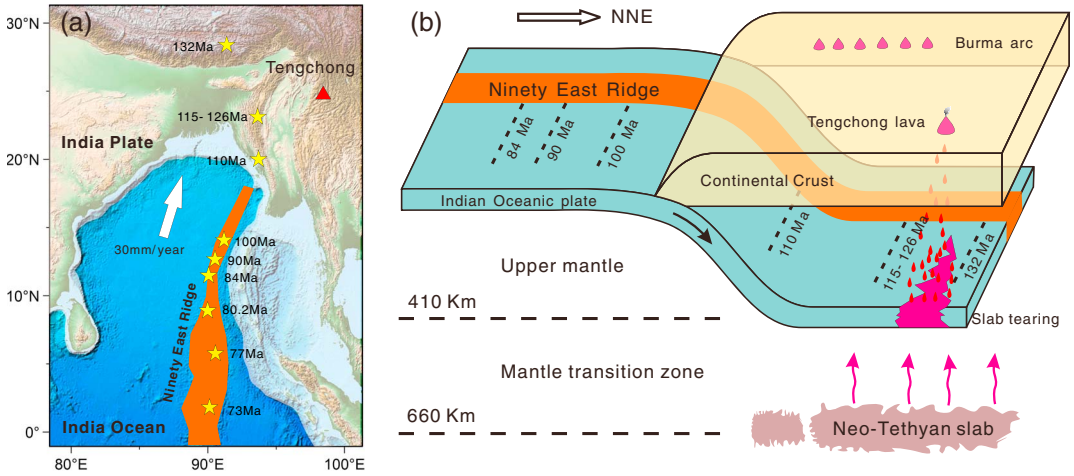

Figure 7. (a) Sketch map showing the Ninetyeast Ridge (orange colored). Volcanic rocks (yellow stars) are fed by the Kerguelen hotspot, and the traces of 73–132 Ma age (D. C. Zhu et al., 2009; Frey et al., 2011; Kent et al., 2002; Seno & Rehman, 2011; Storey et al., 1989; Xia et al., 2014) are showed. White thick arrow denotes the direction of India Oceanic plate, and the velocity is shown on the side of arrow. (b) Schematic tectonic setting showing the origin of Tengchong lava. The traces of 115–126 Ma age are located nearly beneath the mantle source of Tengchong. At about 5 Ma, a big change in plate motions would lead to ridge tearing and partial melting of the mantle.

Xia et al., 2014), meaning that the Cretaceous carbonates might have a contribution to the light Ca isotopic composition. This is consistent with the published data that carbonates have relatively low $\delta^{44/40}$Ca during the Cretaceous (Farkaš, Böhm, et al., 2007).

Meanwhile, there was a major change in plate motions in the southeastern Tibetan Plateau at about 5 Ma (Hall, 2002; Lee & Lawver, 1995). This tectonic change could lead to a tear of Indian Oceanic crust and the extensional environment of the Burma–Tengchong terrane, consistent with the distributed extension-induced normal or strike-slip faults in Tengchong volcanic field (Figure 1). More importantly, R. Zhang et al. (2017) proposed that Tengchong volcanoes may originate from slab tearing of the subducting Indian plate in the upper mantle (Figure 7). Consequently, we propose that the ancient marine carbonates are most likely derived from the Indian Oceanic crust.

6. Conclusions

We report high-precision Mg and Ca isotopic compositions for the volcanic rocks in Tengchong, southeastern Tibetan Plateau. The volcanic rocks show lower δ^{26}Mg (−0.31 to −0.38‰) and $\delta^{44/40}$Ca (0.67 to 0.80‰) than primitive mantle (−0.25 ± 0.07‰ and 0.94 ± 0.05‰, respectively), which may indicate the incorporation of carbonate-bearing sediments in the mantle source region. The negative relationships between ε_{Nd} and Th/Nd and Th/Nb, the ultra-high Th/U (8.5–10.5), high Th/Yb (5–13), and low Ba/La (11–15) of volcanic rocks suggest that the mantle was metasomatized by aqueous melts derived from recycled components. Mg and Ca isotopes did not fractionate during cal-alkaline magmatic process, since no correlations are observed in the plots of δ^{26}Mg and $\delta^{44/40}$Ca versus SiO_2 contents and trace element abundance ratios (e.g., Sm/Yb and Ba/Y). Mg–Ca isotopes modeling illustrates that 5–8% recycled carbonates are incorporated into the mantle source through aqueous melt metasomatism. Combined with the geophysical data and the tectonic evolution of Tengchong, we propose that carbonates are probably derived from the Indian Oceanic crust.

Acknowledgments
We thank Ya-jun An and Sha Chen for help during sample analysis and Li-peng Zhang, Kai Wu, Rui-fang Huang, Chan-chan Zhang, and Sai-jun Sun for discussion. We are grateful to two anonymous reviewers whose constructive suggestions greatly improved this manuscript. This work was supported by the Strategic Priority Research Program (B) of the Chinese Academy of Sciences (XDB18000000), National Natural Science Foundation of China (no. 41373007, 91328204), and State Key Laboratory of Geological Processes and Mineral Resources (GPMR201708). Isotopic data are presented in the main text, and major and trace elements data are available in Table S3 in the supporting information.

References

Alt, J. C., & Teagle, D. A. (1999). The uptake of carbon during alteration of ocean crust. *Geochimica et Cosmochimica Acta*, *63*(10), 1527–1535. https://doi.org/10.1016/S0016-7037(99)00123-4

Amini, M., Eisenhauer, A., Böhm, F., Holmden, C., Kreissig, K., Hauff, F., & Jochum, K. P. (2009). Calcium isotopes ($\delta^{44/40}$Ca) in MPI-DING reference glasses, USGS rock powders and various rocks: Evidence for Ca isotope fractionation in terrestrial silicates. *Geostandards and Geoanalytical Research*, *33*(2), 231–247. https://doi.org/10.1111/j.1751-908X.2009.00903.x

An, Y., Wu, F., Xiang, Y., Nan, X., Yu, X., Yang, J., … Huang, F. (2014). High-precision Mg isotope analyses of low-Mg rocks by MC-ICP-MS. *Chemical Geology*, *390*, 9–21. https://doi.org/10.1016/j.chemgeo.2014.09.014

Berner, R. A., Lasaga, A. C., & Garrels, R. M. (1983). The carbonate-silicate geochemical cycle and its effect on atmospheric carbon dioxide over the past 100 million years. *American Journal of Science*, *283*(7), 641–683. https://doi.org/10.2475/ajs.283.7.641

Bizimis, M., Salters, V. J., & Dawson, J. B. (2003). The brevity of carbonatite sources in the mantle: Evidence from Hf isotopes. *Contributions to Mineralogy and Petrology*, *145*(3), 281–300. https://doi.org/10.1007/s00410-003-0452-3

Bourdon, B., Tipper, E. T., Fitoussi, C., & Stracke, A. (2010). Chondritic Mg isotope composition of the Earth. *Geochimica et Cosmochimica Acta*, *74*(17), 5069–5083. https://doi.org/10.1016/j.gca.2010.06.008

Chen, T. F. (2003). The petrology of the volcanic rocks in Tengchong, Yunnan (in Chinese with English abstract). *Sedimentary Geology and Tethyan Geology*, *23*, 56–61.

Chen, F., Satir, M., Ji, J., & Zhong, D. (2002). Nd–Sr–Pb isotopes of Tengchong Cenozoic volcanic rocks from western Yunnan, China: Evidence for an enriched-mantle source. *Journal of Asian Earth Sciences*, *21*(1), 39–45. https://doi.org/10.1016/S1367-9120(02)00007-X

Chen, J. L., Xu, J. F., Kang, Z. Q., & Jie, L. (2010). Origin of Cenozoic alkaline potassic volcanic rocks at KonglongXiang, Lhasa terrane, Tibetan Plateau: Products of partial melting of a mafic lower-crustal source? *Chemical Geology*, *273*(3-4), 286–299. https://doi.org/10.1016/j.chemgeo.2010.03.003

Dasgupta, R., & Hirschmann, M. M. (2010). The deep carbon cycle and melting in Earth's interior. *Earth and Planetary Science Letters*, *298*(1-2), 1–13. https://doi.org/10.1016/j.epsl.2010.06.039

Dasgupta, R., Hirschmann, M. M., & Withers, A. C. (2004). Deep global cycling of carbon constrained by the solidus of anhydrous, carbonated eclogite under upper mantle conditions. *Earth and Planetary Science Letters*, *227*(1-2), 73–85. https://doi.org/10.1016/j.epsl.2004.08.004

DePaolo, D. J. (2004). Calcium isotopic variations produced by biological, kinetic, radiogenic and nucleosynthetic processes. *Reviews in Mineralogy and Geochemistry*, *55*(1), 255–288. https://doi.org/10.2138/gsrmg.55.1.255

Ewing, S. A., Yang, W., DePaolo, D. J., Michalski, G., Kendall, C., Stewart, B. W., … Amundson, R. (2008). Non-biological fractionation of stable Ca isotopes in soils of the Atacama Desert, Chile. *Geochimica et Cosmochimica Acta*, *72*(4), 1096–1110. https://doi.org/10.1016/j.gca.2007.10.029

Fantle, M. S. (2015). Calcium isotopic evidence for rapid recrystallization of bulk marine carbonates and implications for geochemical proxies. *Geochimica et Cosmochimica Acta*, *148*, 378–401. https://doi.org/10.1016/j.gca.2014.10.005

Fantle, M. S., & DePaolo, D. J. (2005). Variations in the marine Ca cycle over the past 20 million years. *Earth and Planetary Science Letters*, *237*(1-2), 102–117. https://doi.org/10.1016/j.epsl.2005.06.024

Fantle, M. S., & Tipper, E. T. (2014). Calcium isotopes in the global biogeochemical Ca cycle: Implications for development of a Ca isotope proxy. *Earth-Science Reviews*, *129*, 148–177. https://doi.org/10.1016/j.earscirev.2013.10.004

Farkaš, J., Böhm, F., Wallmann, K., Blenkinsop, J., Eisenhauer, A., Van Geldern, R., … Veizer, J. (2007). Calcium isotope record of Phanerozoic oceans: Implications for chemical evolution of seawater and its causative mechanisms. *Geochimica et Cosmochimica Acta*, *71*(21), 5117–5134. https://doi.org/10.1016/j.gca.2007.09.004

Farkaš, J., Buhl, D., Blenkinsop, J., & Veizer, J. (2007). Evolution of the oceanic calcium cycle during the late Mesozoic: Evidence from delta Ca-44/40 of marine skeletal carbonates. *Earth and Planetary Science Letters*, *253*(1-2), 96–111. https://doi.org/10.1016/j.epsl.2006.10.015

Frey, F. A., Pringle, M., Meleney, P., Huang, S., & Piotrowski, A. (2011). Diverse mantle sources for Ninetyeast Ridge magmatism: Geochemical constraints from basaltic glasses. *Earth and Planetary Science Letters*, *303*(3-4), 215–224. https://doi.org/10.1016/j.epsl.2010.12.051

Galy, A., Yoffe, O., Janney, P. E., Williams, R. W., Cloquet, C., Alard, O., … Carignan, J. (2003). Magnesium isotope heterogeneity of the isotopic standard SRM980 and new reference materials for magnesium-isotope-ratio measurements. *Journal of Analytical Atomic Spectrometry*, *18*(11), 1352–1356. https://doi.org/10.1039/B309273a

Gao, J. F., Zhou, M. F., Robinson, P. T., Wang, C. Y., Zhao, J. H., & Malpas, J. (2015). Magma mixing recorded by Sr isotopes of plagioclase from dacites of the Quaternary Tengchong volcanic field, SE Tibetan Plateau. *Journal of Asian Earth Sciences*, *98*, 1–17. https://doi.org/10.1016/j.jseaes.2014.10.036

Green, D. H. (1973). Experimental melting studies on a model upper mantle composition at high pressure under water-saturated and water-undersaturated conditions. *Earth and Planetary Science Letters*, *19*(1), 37–53. https://doi.org/10.1016/0012-821x(73)90176-3

Griffith, E. M., Fantle, M. S., Eisenhauer, A., Paytan, A., & Bullen, T. D. (2015). Effects of ocean acidification on the marine calcium isotope record at the Paleocene–Eocene Thermal Maximum. *Earth and Planetary Science Letters*, *419*, 81–92. https://doi.org/10.1016/j.epsl.2015.03.010

Guo, Z., Cheng, Z., Zhang, M., Zhang, L., Li, X., & Liu, J. (2015). Post-collisional high-K calc-alkaline volcanism in Tengchong volcanic field, SE Tibet: Constraints on Indian eastward subduction and slab detachment. *Journal of the Geological Society*, *172*(5), 624–640. https://doi.org/10.1144/jgs2014-078

Hafkenscheid, E., Wortel, M. J. R., & Spakman, W. (2006). Subduction history of the Tethyan region derived from seismic tomography and tectonic reconstructions. *Journal of Geophysical Research*, *111*, B08401. https://doi.org/10.1029/2005JB003791

Hall, R. (2002). Cenozoic geological and plate tectonic evolution of SE Asia and the SW Pacific: Computer-based reconstructions, model and animations. *Journal of Asian Earth Sciences*, *20*(4), 353–431. https://doi.org/10.1016/S1367-9120(01)00069-4

Handler, M. R., Baker, J. A., Schiller, M., Bennett, V. C., & Yaxley, G. M. (2009). Magnesium stable isotope composition of Earth's upper mantle. *Earth and Planetary Science Letters*, *282*(1-4), 306–313. https://doi.org/10.1016/j.epsl.2009.03.031

Hawkesworth, C. J., Turner, S. P., McDermott, F., Peate, D. W., & Van Calsteren, P. (1997). U–Th isotopes in arc magmas: Implications for element transfer from the subducted crust. *Science*, *276*(5312), 551–555. https://doi.org/10.1126/science.276.5312.551

Heuser, A., Eisenhauer, A., Gussone, N., Bock, B., Hansen, B. T., & Nägler, T. F. (2002). Measurement of calcium isotopes (delta Ca-44) using a multicollector TIMS technique. *International Journal of Mass Spectrometry*, *220*(3), 385–397. https://doi.org/10.1016/S1387-3806(02)00838-2

Hindshaw, R. S., Bourdon, B., von Strandmann, P. A. P., Vigier, N., & Burton, K. W. (2013). The stable calcium isotopic composition of rivers draining basaltic catchments in Iceland. *Earth and Planetary Science Letters*, *374*, 173–184. https://doi.org/10.1016/j.epsl.2013.05.038

Hoernle, K., Tilton, G., Le Bas, M. J., Duggen, S., & Garbe-Schönberg, D. (2002). Geochemistry of oceanic carbonatites compared with continental carbonatites: Mantle recycling of oceanic crustal carbonate. *Contributions to Mineralogy and Petrology*, *142*(5), 520–542. https://doi.org/10.1007/s004100100308

Holmden, C., & Bélanger, N. (2010). Ca isotope cycling in a forested ecosystem. *Geochimica et Cosmochimica Acta*, *74*(3), 995–1015. https://doi.org/10.1016/j.gca.2009.10.020

Huang, S., Farkaš, J., & Jacobsen, S. B. (2010). Calcium isotopic fractionation between clinopyroxene and orthopyroxene from mantle peridotites. *Earth and Planetary Science Letters*, *292*(3-4), 337–344. https://doi.org/10.1016/j.epsl.2010.01.042

Huang, S., Farkaš, J., & Jacobsen, S. B. (2011). Stable calcium isotopic compositions of Hawaiian shield lavas: Evidence for recycling of ancient marine carbonates into the mantle. *Geochimica et Cosmochimica Acta*, *75*(17), 4987–4997.

Huang, K. J., Teng, F. Z., Wei, G. J., Ma, J. L., & Bao, Z. Y. (2012). Adsorption- and desorption-controlled magnesium isotope fractionation during extreme weathering of basalt in Hainan Island, China. *Earth and Planetary Science Letters*, *359-360*, 73–83. https://doi.org/10.1016/j.epsl.2012.10.007

Huang, X. W., Zhou, M. F., Wang, C. Y., Robinson, P. T., Zhao, J. H., & Qi, L. (2013). Chalcophile element constraints on magma differentiation of Quaternary volcanoes in Tengchong, SW China. *Journal of Asian Earth Sciences*, *76*, 1–11. https://doi.org/10.1016/j.jseaes.2013.07.020

Huang, Z., Wang, P., Xu, M., Wang, L., Ding, Z., Wu, Y., … Li, H. (2015). Mantle structure and dynamics beneath SE Tibet revealed by new seismic images. *Earth and Planetary Science Letters*, *411*, 100–111. https://doi.org/10.1016/j.epsl.2014.11.040

Jacobson, A. D., Andrews, M. G., Lehn, G. O., & Holmden, C. (2015). Silicate versus carbonate weathering in Iceland: New insights from Ca isotopes. *Earth and Planetary Science Letters*, *416*, 132–142. https://doi.org/10.1016/j.epsl.2015.01.030

Jaques, A. L., & Green, D. H. (1980). Anhydrous melting of peridotite at 0–15 Kb pressure and the genesis of tholeiitic basalts. *Contributions to Mineralogy and Petrology*, *73*(3), 287–310. https://doi.org/10.1007/bf00381447

Johnson, E. R., Wallace, P. J., Delgado Granados, H., Manea, V. C., Kent, A. J., Bindeman, I. N., & Donegan, C. S. (2009). Subduction-related volatile recycling and magma generation beneath Central Mexico: Insights from melt inclusions, oxygen isotopes and geodynamic models. *Journal of Petrology*, *50*(9), 1729–1764. https://doi.org/10.1093/petrology/egp051

Kang, J. T., Zhu, H. L., Liu, Y. F., Liu, F., Wu, F., Hao, Y. T., … Huang, F. (2016). Calcium isotopic composition of mantle xenoliths and minerals from eastern China. *Geochimica et Cosmochimica Acta*, *174*, 335–344. https://doi.org/10.1016/j.gca.2015.11.039

Kang, J. T., Ionov, D. A., Liu, F., Zhang, C. L., Golovin, A. V., Qin, L. P., … Huang, F. (2017). Calcium isotopic fractionation in mantle peridotites by melting and metasomatism and Ca isotope composition of the bulk silicate earth. *Earth and Planetary Science Letters*, *474*, 128–137. https://doi.org/10.1016/j.epsl.2017.05.035

Ke, S., Teng, F. Z., Li, S. G., Gao, T., Liu, S. A., He, Y., & Mo, X. (2016). Mg, Sr, and O isotope geochemistry of syenites from northwest Xinjiang, China: Tracing carbonate recycling during Tethyan oceanic subduction. *Chemical Geology*, *437*, 109–119. https://doi.org/10.1016/j.chemgeo.2016.05.002

Kelemen, P. B., & Manning, C. E. (2015). Reevaluating carbon fluxes in subduction zones, what goes down, mostly comes up. *Proceedings of the National Academy of Sciences*, *112*(30), E3997–E4006. https://doi.org/10.1073/pnas.1507889112

Kelemen, P. B., Hanghøj, K., & Greene, A. R. (2003). One view of the geochemistry of subduction-related magmatic arcs, with an emphasis on primitive andesite and lower crust. *Treatise on geochemistry*, *3*, 659.

Kent, R. W., Pringle, M. S., Müller, R. D., Saunders, A. D., & Ghose, N. C. (2002). $^{40}Ar/^{39}Ar$ geochronology of the Rajmahal basalts, India, and their relationship to the Kerguelen Plateau. *Journal of Petrology*, *43*(7), 1141–1153. https://doi.org/10.1093/petrology/43.7.1141

Kerrick, D. M., & Connolly, J. A. D. (2001). Metamorphic devolatilization of subducted oceanic metabasalts: Implications for seismicity, arc magmatism and volatile recycling. *Earth and Planetary Science Letters*, *189*(1-2), 19–29. https://doi.org/10.1016/S0012-821X(01)00347-8

Kushiro, I. (1975). Carbonate-silicate reactions at high pressures and possible presence of dolomite and magnesite in the upper mantle. *Earth and Planetary Science Letters*, *28*(2), 116–120. https://doi.org/10.1016/0012-821X(75)90218-6

Lee, T. Y., & Lawver, L. A. (1995). Cenozoic plate reconstruction of Southeast Asia. *Tectonophysics*, *251*(1-4), 85–138. https://doi.org/10.1016/0040-1951(95)00023-2

Lei, J., Zhao, D., & Su, Y. (2009). Insight into the origin of the Tengchong intraplate volcano and seismotectonics in southwest China from local and teleseismic data. *Journal of Geophysical Research*, *114*, B05302. https://doi.org/10.1029/2008JB005881

Lei, J., Xie, F., Fan, Q., & Santosh, M. (2013). Seismic imaging of the deep structure under the Chinese volcanoes: An overview. *Physics of the Earth and Planetary Interiors*, *224*, 104–123. https://doi.org/10.1016/j.pepi.2013.08.008

Li, X., & Liu, J. Q. (2012). A study on the geochemical characteristics and petrogenesis of Holocene volcanic rocks in the Tengchong volcanic eruption field, Yunnan Province, SW China. *Acta Petrologica Sinica*, *28*(5), 1507–1516.

Li, W. Y., Teng, F. Z., Ke, S., Rudnick, R. L., Gao, S., Wu, F. Y., & Chappell, B. W. (2010). Heterogeneous magnesium isotopic composition of the upper continental crust. *Geochimica et Cosmochimica Acta*, *74*(23), 6867–6884. https://doi.org/10.1016/j.gca.2010.08.030

Li, W. Y., Teng, F. Z., Wing, B. A., & Xiao, Y. (2014). Limited magnesium isotope fractionation during metamorphic dehydration in metapelites from the Onawa contact aureole Maine. *Geochemistry, Geophysics, Geosystems*, *15*, 408–415. https://doi.org/10.1002/2013GC004992

Li, S. G., Yang, W., Ke, S., Meng, X., Tian, H., Xu, L., … Sun, W. (2017). Deep carbon cycles constrained by a large-scale mantle Mg isotope anomaly in eastern China. *National Science Review*, *4*(1), nww070–nww120. https://doi.org/10.1093/nsr/nww070

Liu, S. A., Teng, F. Z., He, Y., Ke, S., & Li, S. (2010). The investigation of magnesium isotope fractionation during granite differentiation. *Earth and Planetary Science Letters*, *297*(3-4), 646–654. https://doi.org/10.1016/j.epsl.2010.07.019

Liu, X. M., Teng, F. Z., Rudnick, R. L., McDonough, W. F., & Cummings, M. L. (2014). Massive magnesium depletion and isotope fractionation in weathered basalts. *Geochimica et Cosmochimica Acta*, *135*, 336–349. https://doi.org/10.1016/j.gca.2014.03.028

Liu, D., Zhao, Z., Zhu, D. C., Niu, Y., DePaolo, D. J., Harrison, T. M., … Zhang, Z. (2014). Postcollisional potassic and ultrapotassic rocks in southern Tibet: Mantle and crustal origins in response to India–Asia collision and convergence. *Geochimica et Cosmochimica Acta*, *143*, 207–231. https://doi.org/10.1016/j.gca.2014.03.031

Liu, D., Zhao, Z., Zhu, D. C., Niu, Y., Widom, E., Teng, F. Z., … Mo, X. (2015). Identifying mantle carbonatite metasomatism through Os–Sr–Mg isotopes in Tibetan ultrapotassic rocks. *Earth and Planetary Science Letters*, *430*, 458–469. https://doi.org/10.1016/j.epsl.2015.09.005

Liu, F., Zhu, H. L., Li, X., Wang, G. Q., & Zhang, Z. F. (2017). Calcium isotopic fractionation and compositions of geochemical reference materials. *Geostandards and Geoanalytical Research*. https://doi.org/10.1111/ggr.12172

McDonough, W. F., & Sun, S. S. (1995). The composition of the Earth. *Chemical Geology*, *120*(3-4), 223–253. https://doi.org/10.1016/0009-2541(94)00140-4

Plank, T., & Langmuir, C. H. (1998). The chemical composition of subducting sediment and its consequences for the crust and mantle. *Chemical Geology*, *145*(3-4), 325–394. https://doi.org/10.1016/S0009-2541(97)00150-2

Pogge von Strandmann, P. A. P., Burton, K. W., James, R. H., van Calsteren, P., Gislason, S. R., & Sigfússon, B. (2008). The influence of weathering processes on riverine magnesium isotopes in a basaltic terrain. *Earth and Planetary Science Letters*, *276*(1-2), 187–197. https://doi.org/10.1016/j.epsl.2008.09.020

Poli, S., Franzolin, E., Fumagalli, P., & Crottini, A. (2009). The transport of carbon and hydrogen in subducted oceanic crust: An experimental study to 5 GPa. *Earth and Planetary Science Letters*, *278*(3-4), 350–360. https://doi.org/10.1016/j.epsl.2008.12.022

Prelević, D., Jacob, D. E., & Foley, S. F. (2013). Recycling plus: A new recipe for the formation of Alpine-Himalayan orogenic mantle lithosphere. *Earth and Planetary Science Letters*, *362*, 187–197. https://doi.org/10.1016/j.epsl.2012.11.035

Richards, A., Argles, T., Harris, N., Parrish, R., Ahmad, T., Darbyshire, F., & Draganits, E. (2005). Himalayan architecture constrained by isotopic tracers from clastic sediments. *Earth and Planetary Science Letters*, *236*(3-4), 773–796. https://doi.org/10.1016/j.epsl.2005.05.034

Rudnick, R., & Gao, S. (2003). Composition of the continental crust. *Treatise on Geochemistry*, *3*, 1–64.

Sekine, T., & Wyllie, P. J. (1983). Experimental simulation of mantle hybridization in subduction zones. *The Journal of Geolog*, *91*(5), 511–528. https://doi.org/10.1086/628802

Seno, T., & Rehman, H. U. (2011). When and why the continental crust is subducted: Examples of Hindu Kush and Burma. *Gondwana Research*, *19*(1), 327–333. https://doi.org/10.1016/j.gr.2010.05.011

Simon, J. I., & DePaolo, D. J. (2010). Stable calcium isotopic composition of meteorites and rocky planets. *Earth and Planetary Science Letters*, *289*(3-4), 457–466. https://doi.org/10.1016/j.epsl.2009.11.035

Skulan, J., DePaolo, D. J., & Owens, T. L. (1997). Biological control of calcium isotopic abundances in the global calcium cycle. *Geochimica et Cosmochimica Acta*, *61*(12), 2505–2510. https://doi.org/10.1016/S0016-7037(97)00047-1

Sleep, N. H., & Zahnle, K. (2001). Carbon dioxide cycling and implications for climate on ancient Earth. *Journal of Geophysical Research*, *106*(E1), 1373–1399. https://doi.org/10.1029/2000JE001247

Storey, M., Saunders, A. D., Tarney, J., Gibson, I. L., Norry, M. J., Thirlwall, M. F., … Menzies, M. A. (1989). Contamination of Indian-Ocean asthenosphere by the Kerguelen–Heard mantle plume. *Nature*, *338*(6216), 574–576. https://doi.org/10.1038/338574a0

Sun, W. D., Bennett, V. C., & Kamenetsky, V. S. (2004). The mechanism of Re enrichment in arc magmas: Evidence from Lau Basin basaltic glasses and primitive melt inclusions. *Earth and Planetary Science Letters*, *222*(1), 101–114. https://doi.org/10.1016/j.epsl.2004.02.011

Teng, F. Z. (2017). Magnesium isotope geochemistry. *Reviews in Mineralogy and Geochemistry*, *82*(1), 219–287. https://doi.org/10.2138/rmg.2017.82.7

Teng, F. Z., Wadhwa, M., & Helz, R. T. (2007). Investigation of magnesium isotope fractionation during basalt differentiation: Implications for a chondritic composition of the terrestrial mantle. *Earth and Planetary Science Letters*, *261*(1-2), 84–92. https://doi.org/10.1016/j.epsl.2007.06.004

Teng, F. Z., Li, W. Y., Rudnick, R. L., & Gardner, L. R. (2010). Contrasting lithium and magnesium isotope fractionation during continental weathering. *Earth and Planetary Science Letters*, *300*(1-2), 63–71. https://doi.org/10.1016/j.epsl.2010.09.036

Teng, F. Z., Li, W. Y., Ke, S., Marty, B., Dauphas, N., Huang, S., … Pourmand, A. (2010). Magnesium isotopic composition of the Earth and chondrites. *Geochimica et Cosmochimica Acta*, *74*(14), 4150–4166. https://doi.org/10.1016/j.gca.2010.04.019

Teng, F. Z., Yang, W., Rudnick, R. L., & Hu, Y. (2013). Heterogeneous magnesium isotopic composition of the lower continental crust: A xenolith perspective. *Geochemistry, Geophysics, Geosystems*, *14*, 3844–3856. https://doi.org/10.1002/Ggge.20238

Teng, F. Z., Li, W. Y., Ke, S., Yang, W., Liu, S. A., Sedaghatpour, F., … Xiao, Y. (2015). Magnesium isotopic compositions of international geological reference materials. *Geostandards and Geoanalytical Research*, *39*(3), 329–339. https://doi.org/10.1111/j.1751-908X.2014.00326.x

Thomson, A. R., Walter, M. J., Kohn, S. C., & Brooker, R. A. (2016). Slab melting as a barrier to deep carbon subduction. *Nature*, *529*(7584), 76–79. https://doi.org/10.1038/nature16174

Tipper, E. T., Galy, A., & Bickle, M. J. (2006). Riverine evidence for a fractionated reservoir of Ca and Mg on the continents: Implications for the oceanic Ca cycle. *Earth and Planetary Science Letters*, *247*(3-4), 267–279. https://doi.org/10.1016/j.epsl.2006.04.033

Tipper, E. T., Galy, A., & Bickle, M. J. (2008). Calcium and magnesium isotope systematics in rivers draining the Himalaya-Tibetan-Plateau region: Lithological or fractionation control? *Geochimica et Cosmochimica Acta*, *72*(4), 1057–1075. https://doi.org/10.1016/j.gca.2007.11.029

Valdes, M. C., Moreira, M., Foriel, J., & Moynier, F. (2014). The nature of Earth's building blocks as revealed by calcium isotopes. *Earth and Planetary Science Letters*, *394*, 135–145. https://doi.org/10.1016/j.epsl.2014.02.052

Van der Voo, R., Spakman, W., & Bijwaard, H. (1999). Tethyan subducted slabs under India. *Earth and Planetary Science Letters*, *171*(1), 7–20. https://doi.org/10.1016/S0012-821X(99)00131-4

Wang, F., Peng, Z., Zhu, R., He, H., & Yang, L. (2006). Petrogenesis and magma residence time of lavas from Tengchong volcanic field (China): Evidence from U series disequilibria and $^{40}Ar/^{39}Ar$ dating. *Geochemistry, Geophysics, Geosystems*, *7*, Q01002. https://doi.org/10.1029/2005GC001023

Wang, S. J., Teng, F. Z., & Li, S. G. (2014). Tracing carbonate–silicate interaction during subduction using magnesium and oxygen isotopes. *Nature Communications*, *5*, 5328. https://doi.org/10.1038/ncomms6328

Wang, S. J., Teng, F. Z., Li, S. G., & Hong, J. A. (2014). Magnesium isotopic systematics of mafic rocks during continental subduction. *Geochimica et Cosmochimica Acta*, *143*, 34–48. https://doi.org/10.1016/j.gca.2014.03.029

Wei, W., Xu, J., Zhao, D., & Shi, Y. (2012). East Asia mantle tomography: New insight into plate subduction and intraplate volcanism. *Journal of Asian Earth Sciences*, *60*, 88–103. https://doi.org/10.1016/j.jseaes.2012.08.001

Williams, R. W., Collerson, K. D., Gill, J. B., & Deniel, C. (1992). High Th/U ratios in subcontinental lithospheric mantle—Mass-spectrometric measurement of Th isotopes in Gaussberg Lamproites. *Earth and Planetary Science Letters*, *111*(2-4), 257–268. https://doi.org/10.1016/0012-821x(92)90183-V

Woodhead, J. D., Hergt, J. M., Davidson, J. P., & Eggins, S. M. (2001). Hafnium isotope evidence for 'conservative' element mobility during subduction zone processes. *Earth and Planetary Science Letters*, *192*(3), 331–346. https://doi.org/10.1016/S0012-821X(01)00453-8

Workman, R. K., & Hart, S. R. (2005). Major and trace element composition of the depleted MORB mantle (DMM). *Earth and Planetary Science Letters*, *231*(1-2), 53–72. https://doi.org/10.1016/j.epsl.2004.12.005

Wu, K., Ling, M. X., Sun, W., Guo, J., & Zhang, C. C. (2017). Major transition of continental basalts in the Early Cretaceous: Implications for the destruction of the North China Craton. *Chemical Geology*, *470*, 93–106. https://doi.org/10.1016/j.chemgeo.2017.08.025

Xia, Y., Zhu, D. C., Wang, Q., Zhao, Z. D., Liu, D., Wang, L. Q., & Mo, X. X. (2014). Picritic porphyrites and associated basalts from the remnant Comei large Igneous Province in SE Tibet: Records of mantle-plume activity. *Terra Nova*, *26*(6), 487–494. https://doi.org/10.1111/ter.12124

Xu, J. F., Castillo, P. R., Li, X. H., Yu, X. Y., Zhang, B. R., & Han, Y. W. (2002). MORB-type rocks from the Paleo-Tethyan Mian-Lueyang northern ophiolite in the Qinling Mountains, central China: Implications for the source of the low $^{206}Pb/^{204}Pb$ and high $^{143}Nd/^{144}Nd$ mantle component in the Indian Ocean. *Earth and Planetary Science Letters*, *198*(3-4), 323–337. https://doi.org/10.1016/S0012-821X(02)00536-8

Yang, W., Teng, F. Z., & Zhang, H. F. (2009). Chondritic magnesium isotopic composition of the terrestrial mantle: A case study of peridotite xenoliths from the North China Craton. *Earth and Planetary Science Letters*, *288*(3-4), 475–482. https://doi.org/10.1016/j.epsl.2009.10.009

Yang, W., Teng, F. Z., Li, W. Y., Liu, S. A., Shan, K., Liu, Y. S., … Gao, S. (2016). Magnesium isotopic composition of the deep continental crust. *American Mineralogist*, *101*(2), 243–252. https://doi.org/10.2138/am-2016-5275

Yu, H., Xu, J., Lin, C., Shi, L., & Chen, X. (2012). Magmatic processes inferred from chemical composition, texture and crystal size distribution of the Heikongshan lavas in the Tengchong volcanic field, SW China. *Journal of Asian Earth Sciences*, *58*, 1–15. https://doi.org/10.1016/j.jseaes.2012.07.013

Zhang, Y. T., Liu, J. Q., & Meng, F. C. (2012). Geochemistry of Cenozoic volcanic rocks in Tengchong, SW China: Relationship with the uplift of the Tibetan Plateau. *Island Arc*, *21*(4), 255–269. https://doi.org/10.1111/j.1440-1738.2012.00819.x

Zhang, R., Wu, Y., Gao, Z., Fu, Y. V., Sun, L., Wu, Q., & Ding, Z. (2017). Upper mantle discontinuity structure beneath eastern and southeastern Tibet: New constraints on the Tengchong intraplate volcano and signatures of detached lithosphere under the western Yangtze Craton. *Journal of Geophysical Research: Solid Earth*, *122*, 1367–1380. https://doi.org/10.1002/2016JB013551

Zhou, M. F., Robinson, P. T., Wang, C. Y., Zhao, J. H., Yan, D. P., Gao, J. F., & Malpas, J. (2012). Heterogeneous mantle source and magma differentiation of quaternary arc-like volcanic rocks from Tengchong, SE margin of the Tibetan Plateau. *Contributions to Mineralogy and Petrology*, *163*(5), 841–860. https://doi.org/10.1007/s00410-011-0702-8

Zhu, B. Q., Mao, C. X., Lugmair, G. W., & Macdougall, J. D. (1983). Isotopic and geochemical evidence for the origin of Plio-Pleistocene volcanic rocks near the Indo-Eurasian collisional margin at Tengchong, China. *Earth and Planetary Science Letters*, *65*(2), 263–275. https://doi.org/10.1016/0012-821X(83)90165-6

Zhu, D. C., Chung, S. L., Mo, X. X., Zhao, Z. D., Niu, Y., Song, B., & Yang, Y. H. (2009). The 132 Ma Comei-Bunbury large igneous province: Remnants identified in present-day southeastern Tibet and southwestern Australia. *Geology*, *37*(7), 583–586. https://doi.org/10.1130/g30001a.1

Zhu, H. L., Zhang, Z. F., Wang, G. Q., Liu, Y. F., Liu, F., Li, X., & Sun, W. D. (2016). Calcium isotopic fractionation during ion-exchange column chemistry and thermal ionisation mass spectrometry (TIMS) determination. *Geostandards and Geoanalytical Research*, *40*(2), 185–194. https://doi.org/10.1111/j.1751-908X.2015.00360.x

Zou, H., Fan, Q., Schmitt, A. K., & Sui, J. (2010). U–Th dating of zircons from Holocene potassic andesites (Maanshan volcano, Tengchong, SE Tibetan Plateau) by depth profiling: Time scales and nature of magma storage. *Lithos*, *118*(1-2), 202–210. https://doi.org/10.1016/j.lithos.2010.05.001

Zou, H., Shen, C. C., Fan, Q., & Lin, K. (2014). U-series disequilibrium in young Tengchong volcanics: Recycling of mature clay sediments or mudstones into the SE Tibetan mantle. *Lithos*, *192–195*, 132–141. https://doi.org/10.1016/j.lithos.2014.01.017